Integrating Hyperspectral and Phenological Features for Cereals Mapping in a Mediterranean Region, Morocco

Mohamed Bourriz [1,2,3], Ahmed Laamrani [1,4,5], Nadir El Bouanani[1,2], Walid Elbarz [2], Hamd Ait Abdelali[2], Francois Bourzeix[2], Abdelghani Chehbouni[1]

[1] Center for Remote Sensing Applications (CRSA), Mohammed VI Polytechnic University (UM6P), Campus Ben Guerir 43150, Morocco – mohamed.bourriz@um6p.ma , Ahmed.LAAMRANI@um6p.ma, nadir.elbouanani@um6p.ma, Abdelghani.CHEHBOUNI@um6p.ma
[2] Analytics Laboratory (A-Lab), UM6P, Campus Rabat 11103, Morocco – walid.ELBARZ@um6p.ma, Hamd.AITABDELALI@um6p.ma, Francois.BOURZEIX@um6p.ma
[3] Friedrich Schiller University Jena, Department of Geography, Jena 07743, Germany
[4] Department of Geography, Environment & Geomatics, University of Guelph, Guelph, ON N1G 2W1, Canada
[5] Institut de recherche sur les forêts (IRF), Université du Québec en Abitibi-Temiscamingue (UQAT), 445 boul. de l'Universite´, Rouyn-Noranda, Québec J9X 5E4, Canada

Keywords: Hyperspectral Imagery, Cereal Crop Mapping, Dynamic Time Warping, Spectral Attention Module, Multimodal Remote Sensing.

Abstract

Accurate mapping of winter cereals in fragmented agricultural landscapes remains challenging, as single-date spectral imagery captures only a snapshot of crop conditions, while temporal approaches alone may miss subtle biochemical and structural differences between crop types. This study proposes a hybrid framework integrating hyperspectral and phenology-informed features for winter cereal mapping in the Saïss Plain, north-central Morocco. A Spectral Attention Module (SAM) was applied to EnMAP hyperspectral imagery to identify 29 informative narrow bands. In a second scenario, these spectral features were complemented with a Dynamic Time Warping (DTW)-based dissimilarity metric derived from Sentinel-2 Enhanced Vegetation Index (EVI) time series, measuring the similarity of each parcel's seasonal profile to a reference winter cereal trajectory. Three classifiers — Random Forest (RF), Support Vector Machine (SVM), and TabPFN — were evaluated using nested random (CV) and spatial cross-validation (SCV) to assess predictive performance and spatial generalization. The hyperspectral-only scenario already achieved high separability, with spatial ROC-AUC values reaching 0.95 for SVM and 0.93 for TabPFN. Adding the DTW-based dissimilarity feature improved robustness, particularly for RF, whose spatial ROC-AUC range shifted from 0.89 (SCV)–0.98 (CV) to 0.91 (SCV)–0.99 (CV). Overall, SVM remained the strongest model in spatial ROC-AUC, while the fused spectral–temporal representation reduced low-performing cases and improved generalization under spatial validation. These findings demonstrate that combining attention-selected hyperspectral bands with a DTW-based temporal similarity metric provides an effective framework for winter cereal mapping in heterogeneous agricultural systems.

1. INTRODUCTION

Accurate and up-to-date crop-type information is crucial for agricultural monitoring, food-security strategies, and sustainable land management, especially in regions dominated by fragmented fields and diverse cropping systems (Ouzemou *et al.*, 2018). In such settings, crop classification remains difficult, as variability within the same class can be considerable, while different crops may show similar spectral signatures on a single acquisition date (Alami Machichi *et al.*, 2022). These limitations are particularly pronounced in semi-arid agricultural regions, where management practices, sowing dates, and local environmental conditions may differ substantially even between neighboring parcels (El Hachimi *et al.*, 2022).

Multispectral time series data, particularly from Sentinel-2, are now widely used for crop mapping, as they capture vegetation changes throughout the growing season. Vegetation indices derived from these data, such as the Enhanced Vegetation Index (EVI), are useful for describing temporal crop development and improving class discrimination. Among time-series analysis methods, Dynamic Time Warping (DTW) has attracted strong interest for its ability to compare seasonal trajectories even when crop development is shifted in time (Belgiu *et al.*, 2020). This characteristic makes DTW especially suitable for heterogeneous farming systems, where growth cycles are rarely synchronized across fields. Previous studies have shown that temporal approaches can outperform single-date imagery, and that DTW-based methods are particularly effective under strong phenological variability (Belgiu and Csillik, 2018; Huang *et al.*, 2024).

At the same time, the availability of spaceborne hyperspectral data as EnMAP and PRISMA has opened new opportunities for crop discrimination (Bourriz, Hajji, *et al.*, 2025). In contrast to multispectral sensors, hyperspectral imagery provides continuous and detailed spectral information, enabling a finer characterization of vegetation properties such as pigment content, water status, canopy structure, and biochemical composition (Thenkabail, Lyon and Huete, 2018). This spectral richness is valuable for separating crop classes that may follow similar seasonal patterns yet differ in their instantaneous spectral response. Nevertheless, hyperspectral datasets are inherently high-dimensional and redundant, making feature selection essential for identifying the most informative wavelengths while reducing noise and complexity (Laamrani *et al.*, 2019; Misbah *et al.*, 2024; Elbouanani *et al.*, 2025). Recent research, including previous work (Aneece and Thenkabail, 2022; Bourriz, Laamrani, *et al.*, 2025) related to this study, has highlighted the potential of EnMAP for crop mapping and the usefulness of compact hyperspectral feature sets in complex agricultural environments.

Another important challenge concerns the reliability of model assessment. Conventional random train-test splits often produce overly optimistic results, as neighboring parcels tend to share similar environmental and management conditions. As a result, models that appear highly accurate under random validation may prove less reliable when transferred to new locations (Schratz *et al.*, 2019). For this reason, spatially explicit validation has become increasingly important for assessing the true robustness and transferability of crop-mapping methods (Peña and Brenning, 2015). This issue is particularly critical in fragmented agricultural landscapes, where spatial autocorrelation can strongly bias random cross-validation when training and testing samples are not geographically separated.

Against this background, the present study examines whether the integration of hyperspectral and temporal information can enhance winter cereal discrimination in the Saïss Plain in Morocco.

Two feature scenarios are investigated. The first relies on EnMAP imagery processed through a Spectral Attention Module (SAM) to identify the most informative narrow bands for classification. The second augments these hyperspectral features with a DTW-based dissimilarity metric derived from Sentinel-2 EVI time series. Rather than explicitly modelling phenology, this temporal feature acts as an implicit phenology-informed similarity descriptor by measuring how closely each parcel’s seasonal trajectory resembles a reference winter cereal profile. The resulting framework was evaluated using Random Forest (RF), Support Vector Machine (SVM), and TabPFN, a recently developed transformer-based foundation model for tabular data (Hollmann *et al.*, 2025), under both random and spatial nested cross-validation to assess predictive performance and spatial generalization.

Accordingly, this study has two main objectives: first, to evaluate the contribution of attention-selected hyperspectral narrow bands for winter cereal mapping; and second, to determine whether the addition of a DTW-derived temporal similarity feature improves class separability and generalization under spatial validation.

2. STUDY AREA AND DATASET

2.1 Study Area and Ground Truth Data

The study was carried out in the Saïss Plain, located in the Fez–Meknès region of north-central Morocco, with a particular focus on the agricultural landscapes surrounding the Aïn Orma commune near Meknès (**Figure 1**).

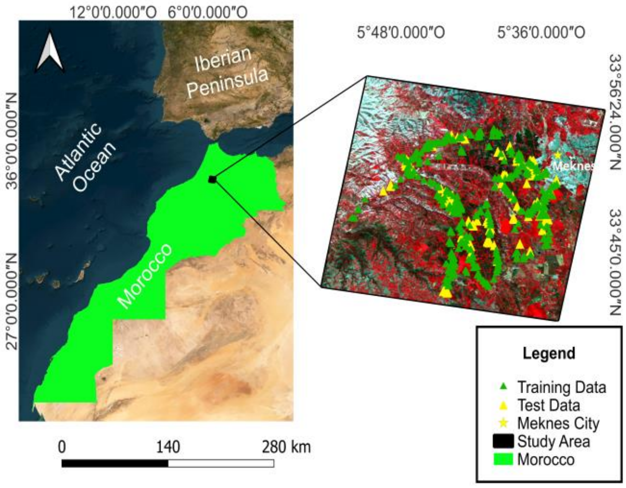

Figure 1. Study Area

The region consists of fertile plains bordered by the piedmonts of the Middle Atlas and Rif Mountains and is considered one of Morocco’s most productive agricultural areas due to its favorable soils and long-established cereal-based farming systems (Bouras *et al.*, 2021; Amazirh *et al.*, 2026). According to regional agricultural statistics, the Fez–Meknès region accounts for nearly 20% of the national cereal production, while cereals occupy approximately 53% of the arable land, mainly including durum wheat, soft wheat, and barley (Belmahi *et al.*, 2023). The climate is Mediterranean semi-arid to sub-humid, with cool and wet winters, hot and dry summers, and annual precipitation ranging from 350 to 550 mm.

Reference data were collected during the 2024–2025 cropping season using QField and were complemented by field visits and farmer interviews. The final dataset consisted of 339 parcel polygons, including 219 winter cereal parcels and 120 parcels belonging to other crop types. For the purpose of this study, the parcels were grouped into two classes: winter cereals and other crops. The winter cereal class included soft wheat, durum wheat, barley, and oats.

2.2 Remote Sensing Data

A single EnMAP hyperspectral image acquired in March 2025 was used as the primary spectral dataset. To ensure consistent reflectance quality, the image was first pre-processed by removing spectral bands affected by atmospheric water absorption and sensor noise, particularly in the SWIR regions between 1320–1500 nm and 1780–2050 nm. The remaining spectra were then smoothed using a Savitzky–Golay filter in order to reduce noise while preserving relevant spectral features. Finally, the EnMAP image was co-registered to a Sentinel-2 acquisition from a nearby date to ensure spatial consistency between the hyperspectral and multispectral datasets.

To complement the hyperspectral information, Sentinel-2 Level-2A imagery was processed using the openEO Python client to derive a temporal Enhanced Vegetation Index (EVI) series representative of crop seasonal dynamics. The Sentinel-2 dataset covered the period from 1 September 2024 to 1 September 2025 and included the blue (B02), red (B04), and near-infrared (B08) bands required for EVI computation. Only scenes with a maximum cloud cover of 15% were retained. Cloud- and shadow-affected pixels were identified using the

Scene Classification Layer (SCL) and masked through a dilation-based procedure implemented in openEO to reduce residual contamination around cloudy areas. After masking, the Sentinel-2 observations were aggregated into decadal (i.e. 10 days) composites using the median reflectance value.. Missing observations were subsequently filled by linear interpolation along the temporal dimension, producing a regular and gap-reduced time series suitable for temporal analysis. The resulting dekadal EVI profiles (**Figure 2**) for each class were then used to characterize crop-season behavior and to derive the DTW-based dissimilarity feature.

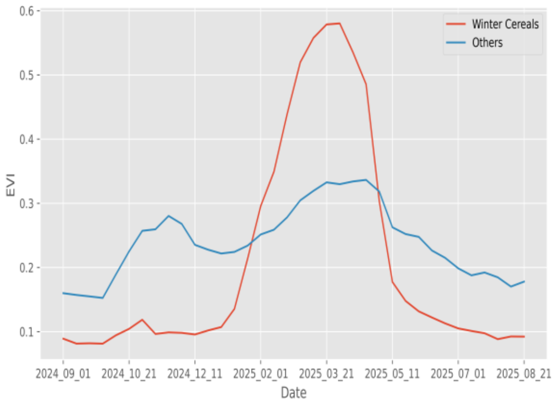

Figure 2.Temporal patterns of EVI for the two classes.

3. METHODOLOGY

The methodology adopted in this study consisted of three main stages (**Figure 3**). First, the EnMAP hyperspectral image was pre-processed through noisy band removal, spectral smoothing, and co-registration, and then analysed using a Spectral Attention Module (SAM) to identify the most relevant spectral bands for winter cereal discrimination based on adaptive wavelength weighting. To obtain a fixed and stable subset of bands while avoiding the additional complexity of repeating the procedure within each fold, feature selection was applied once as a preprocessing step prior to cross-validation. Second, Sentinel-2 (EVI)-based time series were generated and compared with a reference winter cereal profile using DTW, producing a dissimilarity feature that captured temporal similarity in crop seasonal behaviour. Third, classification was conducted under two experimental settings: Scenario 1, using the selected hyperspectral bands only, and Scenario 2, combining the selected hyperspectral bands with the DTW-based dissimilarity feature after alignment and concatenation. In both cases, SVM, Random Forest, and TabPFN classifiers were trained and optimized using repeated nested random and spatial cross-validation, where the inner loop was used for model selection, and the outer loop was used to obtain an unbiased estimate of predictive performance; in the spatial setting, folds were defined using K-means-based spatial grouping.. The resulting performance was then used to compare the contribution of hyperspectral information alone against the added value of integrating the DTW-derived temporal metric.

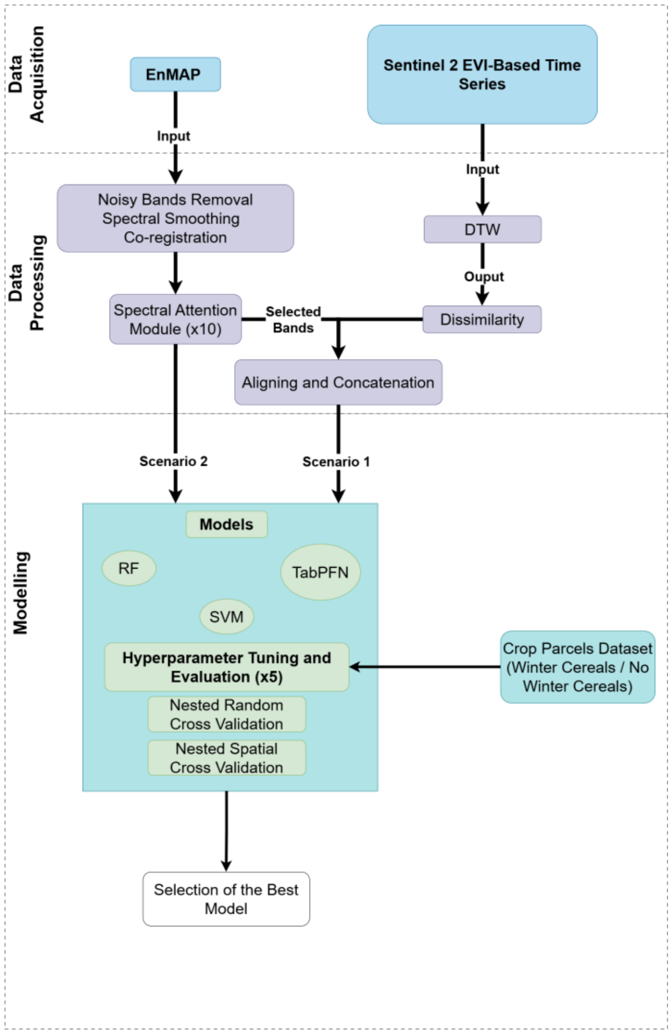

Figure 3. Methodological workflow.

3.1 Spectral Attention Module

To identify the most informative hyperspectral wavelengths for winter cereal discrimination, a Spectral Attention Module (SAM) (**Figure 4**), inspired by Squeeze-and-Excitation networks, was applied to the EnMAP spectral data. The module estimates band-wise attention scores using two fully connected layers with a reduction ratio of 16, followed by a sigmoid activation, while L1 regularization was introduced to encourage sparsity in the learned weights. These attention scores act as soft selectors, emphasizing relevant wavelengths and attenuating less informative ones. To improve the stability of the selection, the procedure was repeated 10 times, and the 29 wavelengths that appeared most consistently across runs were retained as the final subset, corresponding to scenario 1 (spectral features only) in the subsequent modelling stage.

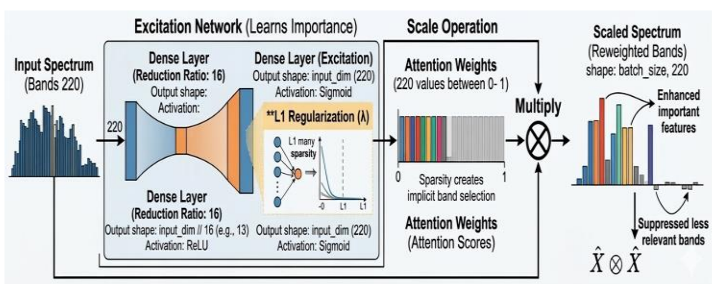

Figure 4. SAM architecture.

This reduced band subset was chosen to address the strong redundancy typically present in hyperspectral imagery, where bands are often highly correlated (Bourriz *et al.*, 2026). Reducing the number of input bands also helps limit model complexity and lowers the risk of performance deterioration in high-dimensional feature spaces. Similar dimensionality-reduction strategies have been reported in previous hyperspectral crop-mapping studies, where compact subsets of informative bands improved computational efficiency while preserving classification performance comparable to that obtained with the full spectrum (Aneece *et al.*, 2024; Bourriz, Laamrani, *et al.*, 2025).

3.2 Dynamic Time Warping (DTW)

To complement the hyperspectral information with a temporal descriptor, a Dynamic Time Warping (DTW)-based dissimilarity metric was derived from the Sentinel-2 Enhanced Vegetation Index (EVI) time series. DTW is a similarity measure designed for temporal sequences and is particularly suitable for crop mapping, as it can align time series that differ in timing, duration, or local phase shifts while preserving their overall seasonal shape. This property makes DTW well suited to agricultural applications, where crop cycles may vary across parcels due to differences in sowing dates, environmental conditions, and management practices.

In this study, EVI was used as the input temporal signal, and a reference winter cereal profile was constructed from the training dataset by computing the median EVI trajectory of parcels labelled as cereal across all available dates. This median profile was then cleaned to remove missing values and used as the temporal template against which all pixel time series were compared. For each target time series, missing observations were linearly interpolated when sufficient valid values were available, and only series with an acceptable proportion of missing data were retained. The implementation adopted here relied on the standard DTW distance, computed directly between the one-dimensional EVI template and each EVI time series, without an additional temporal weighting constraint. This choice was considered appropriate for the present study, which focused on a binary classification problem (winter cereals versus other crops). However, future work could extend this approach by incorporating time-weighted DTW formulations, which may be particularly beneficial in multi-class settings, where finer temporal distinctions between several crop types become more important (Belgiu and Csillik, 2018). After spatial alignment with the EnMAP data, the DTW-derived dissimilarity metric was normalized prior to feature fusion and then concatenated with the selected spectral bands to serve as the additional input in the fused classification scenario.

3.3 Model Assessment

To evaluate the classification performance of the two feature scenarios, SVM, Random Forest (RF), and the specialized deep learning model Tabular Prior-Data Fitted Network (TabPFN) were implemented following the workflow illustrated in **Figure 3**. Model development relied on five repeated nested cross-validation runs, with an inner loop dedicated to hyperparameter tuning and an outer loop used for performance estimation.

Two validation strategies were adopted: nested random cross-validation and nested spatial cross-validation. In the random scheme, samples were partitioned without considering their geographic location. In contrast, the spatial scheme used K-means clustering on parcel coordinates so that each fold corresponded to a geographically distinct subset. This spatial partitioning helps reduce the effect of spatial autocorrelation between training and validation samples and provides a more realistic estimate of model performance under spatial extrapolation (Ruß and Brenning, 2010; Meyer *et al.*, 2019).

The three classifiers were evaluated under both feature scenarios, namely selected hyperspectral bands only and selected hyperspectral bands combined with the DTW-based dissimilarity metric. Performance was assessed using overall accuracy (OA), macro-F1 score, and Receiver Operating Characteristic Area Under the Curve (ROC-AUC). Particular emphasis was given to ROC-AUC, as it provides a threshold-independent measure of class separability and is especially relevant in the presence of class imbalance.

4. RESULTS AND DISCUSSION

The SAM produced a ranked importance profile of the EnMAP spectral bands, making it possible to identify the spectral regions that contributed most to winter cereal discrimination. As shown in Figure 5, the highest attention weights were consistently assigned to bands located in the green region (around 550 nm), the red-edge interval (approximately 700–750 nm), the near-infrared plateau (800–1250 nm), and selected portions of the shortwave infrared (1500–1750 nm and 2000–2400 nm). These spectral domains are commonly linked to vegetation pigment content, canopy structure, biomass, water status, and biochemical composition. Based on the stability of the attention scores across repeated runs, a subset of 29 EnMAP bands was retained as the final set of discriminative spectral features for the hyperspectral-only scenario.

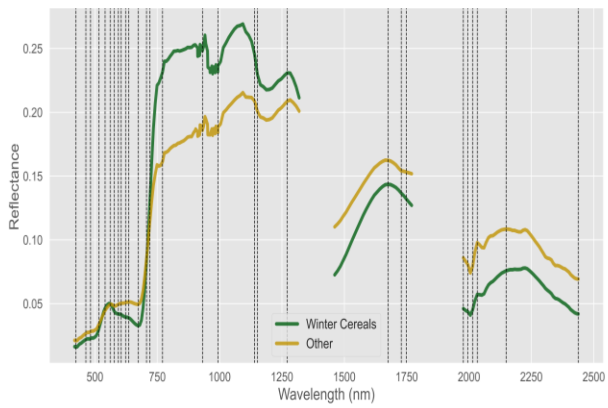

Figure 5. Selected EnMAP bands.

The distribution of the selected bands is consistent with previous findings in hyperspectral crop-mapping studies, which have highlighted the importance of visible, red-edge, near-infrared, and shortwave infrared wavelengths for distinguishing crop types (Aneece and Thenkabail, 2021; Bourriz, Laamrani, *et al.*, 2025). This agreement suggests that the SAM successfully identified physically meaningful spectral regions relevant to winter cereal discrimination, while also reducing the redundancy typically present in hyperspectral datasets.

In parallel, the DTW-based dissimilarity metric derived from Sentinel-2 EVI time series revealed a clear temporal contrast between the two classes (**Figure 6**). Parcels belonging to the winter cereal class showed markedly lower dissimilarity values and a more compact distribution, indicating strong agreement with the reference winter cereal seasonal profile. By contrast, the other crop class exhibited higher median dissimilarity values, a broader interquartile range, and a larger number of extreme values, reflecting greater temporal variability and weaker similarity to the cereal temporal pattern. Although a limited overlap between the two classes remained, the overall separation demonstrates that the DTW-derived feature captured meaningful differences in seasonal behaviour.

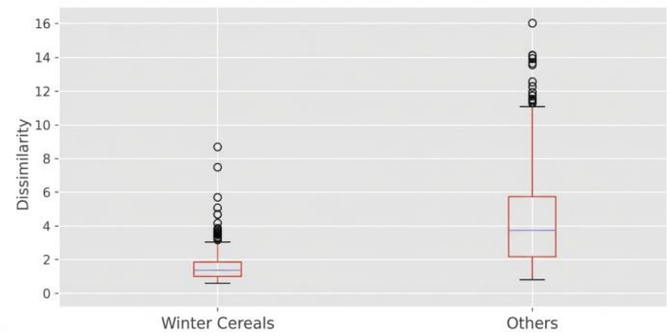

Figure 6. Dissimilarity measure of the two classes.

These results indicate that the DTW dissimilarity metric provides complementary temporal information that is not directly represented in the single-date EnMAP image.

Across all experiments, the results indicate that both the feature configuration and the validation strategy strongly affected classification performance (**Figure 7**). In the HSI-only scenario, the three classifiers achieved consistently high scores under random cross-validation, with mean accuracies of 0.95 for RF, 0.97 for SVM, and 0.99 for TabPFN, while ROC-AUC values were close to or equal to 1.00. In contrast, performance declined substantially under spatial cross-validation, where accuracy dropped to 0.83, 0.86, and 0.80 for RF, SVM, and TabPFN, respectively. Similar reductions were observed for macro-F1 and ROC-AUC. This discrepancy highlights the extent to which random cross-validation can overestimate model generalization in spatially structured agricultural datasets, likely due to the presence of spatially autocorrelated samples in both training and validation folds. By enforcing geographic separation, spatial cross-validation provides a more realistic assessment of model transferability.

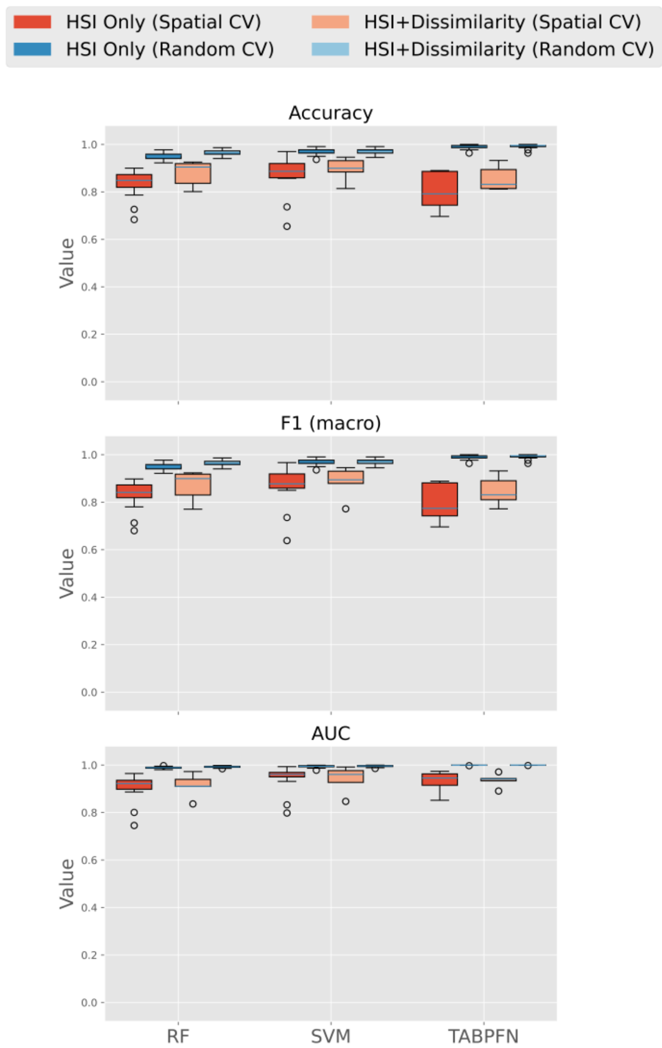

Figure 7. Comparison of model performance with and without dissimilarity metric under random and spatial cross validation.

Among the three used classifiers in this study, SVM was the most stable in the HSI-only setting, achieving the best performance under spatial cross-validation with an accuracy of 0.86, a macro-F1 of 0.85, and a ROC-AUC of 0.93. RF showed comparable macro-F1 performance (0.83), although with greater variability across folds, as indicated by the wider interquartile ranges in Figure 6. TabPFN, despite reaching near-perfect results under random cross-validation (accuracy = 0.99, ROC-AUC = 1.00), exhibited the weakest performance under spatial cross-validation (accuracy=0.80, macro-F1=0.80). This suggests that although TabPFN fitted the in-distribution data very well, its generalization to spatially independent folds was more limited. Overall, these results confirm that the selected hyperspectral bands carry strong discriminative information for winter cereal mapping, while also showing that their spatial transferability varies depending on the classifier.

When the DTW-based dissimilarity feature was added to the hyperspectral input, classification performance improved for all three models, with the clearest gains observed under spatial cross-validation. RF accuracy increased from 0.83 to 0.88, with ROC-AUC rising from 0.89 to 0.91. For SVM, accuracy improved from 0.86 to 0.90, while ROC-AUC increased from 0.93 to 0.94. TabPFN also showed a notable improvement, with accuracy increasing from 0.80 to 0.86 and ROC-AUC from 0.93 to 0.94. These improvements indicate that the dissimilarity feature contributed complementary temporal information beyond the single-date hyperspectral reflectance, thereby improving robustness to spatial variability. Under random cross-validation, by contrast, performance gains were marginal, with all models already operating close to the performance ceiling in the HSI-only scenario. This further illustrates that random cross-validation is less informative for detecting meaningful improvements in spatial generalization.

Overall, RF and TabPFN showed the largest relative gains after integrating the dissimilarity feature, whereas SVM maintained the strongest absolute performance across both scenarios. These findings suggest that combining selected hyperspectral bands with a DTW-derived temporal dissimilarity metric yields a more robust and spatially transferable framework for winter cereal classification, particularly for models whose spatial performance was more limited when relying on hyperspectral information alone.

5. CONCLUSION

This study evaluated a hybrid spectral–temporal framework for winter cereal mapping in the Saïss region of Morocco by combining EnMAP hyperspectral imagery with a Dynamic Time Warping (DTW)-based dissimilarity metric derived from Sentinel-2 Enhanced Vegetation Index (EVI) time series. The results showed that the selected EnMAP bands alone already provided strong discriminatory power for separating winter cereals from other crops. However, the integration of the DTW-based temporal descriptor further improved classification performance, particularly under spatial cross-validation, where a more realistic assessment of model generalization was obtained. This confirms that the temporal dissimilarity feature contributed complementary information beyond the single-date hyperspectral observation.

Among the evaluated classifiers, SVM showed the most stable overall performance, while RF and TabPFN benefited most clearly from the addition of the dissimilarity feature. The comparison between random and spatial cross-validation also highlighted the importance of using geographically explicit validation strategies in fragmented agricultural landscapes, as random cross-validation tended to produce overly optimistic estimates. In this respect, the study demonstrates that combining attention-selected hyperspectral bands with an implicit phenology-informed temporal similarity metric provides a compact and effective framework for winter cereal mapping.

Beyond the present study area, the proposed approach can have good potential for application to other agricultural regions and crop types (i.e., cereals varieties, vegetables, tree-fruit). Its main components are most probably transferable, provided that local reference data are available to derive representative crop-specific temporal profiles and to recalibrate the feature space to local agronomic conditions. Future work could therefore explore the extension of this framework to multi-class crop mapping, the use of time-weighted DTW variants, and the evaluation of its robustness across different seasons and agroecological contexts.

Acknowledgements

This work was conducted within the Yield Gap project (OCP Foundation–UM6P agreement) and made use of EnMAP data provided by and the German Aerospace Center (DLR).

References

Alami Machichi, M. *et al.* (2022) “CerealNet: A Hybrid Deep Learning Architecture for Cereal Crop Mapping Using Sentinel-2 Time-Series,” *Informatics*, 9(4), p. 96. Available at: https://doi.org/10.3390/informatics9040096.

Amazirh, A. *et al.* (2026) “Seasonal field-scale wheat yield forecasting using XGBoost with radar, optical, and weather data in Morocco,” *International Journal of Applied Earth Observation and Geoinformation*, 149, p. 105242. Available at: https://doi.org/10.1016/j.jag.2026.105242.

Aneece, I. *et al.* (2024) “Machine Learning and New-Generation Spaceborne Hyperspectral Data Advance Crop Type Mapping,” *Photogrammetric Engineering & Remote Sensing*, 90(11), pp. 687–698. Available at: https://doi.org/10.14358/PERS.24-00026R2.

Aneece, I. and Thenkabail, P. (2021) “Classifying Crop Types Using Two Generations of Hyperspectral Sensors (Hyperion and DESIS) with Machine Learning on the Cloud,” *REMOTE SENSING*, 13(22). Available at: https://doi.org/10.3390/rs13224704.

Aneece, I. and Thenkabail, P.S. (2022) “New Generation Hyperspectral Sensors DESIS and PRISMA Provide Improved Agricultural Crop Classifications,” *Photogrammetric Engineering and Remote Sensing*, 88(11), pp. 715–729. Available at: https://doi.org/10.14358/PERS.22-00039R2.

Belgiu, M. *et al.* (2020) “DYNAMIC TIME WARPING FOR CROPS MAPPING,” *The International Archives of the Photogrammetry, Remote Sensing and Spatial Information Sciences*, XLIII-B3-2020, pp. 947–951. Available at: https://doi.org/10.5194/isprs-archives-XLIII-B3-2020-947-2020.

Belgiu, M. and Csillik, O. (2018) “Sentinel-2 cropland mapping using pixel-based and object-based time-weighted dynamic time warping analysis,” *Remote Sensing of Environment*, 204, pp. 509–523. Available at: https://doi.org/10.1016/j.rse.2017.10.005.

Belmahi, M. *et al.* (2023) “Analysis of Relationship between Grain Yield and NDVI from MODIS in the Fez-Meknes Region, Morocco,” *Remote Sensing*, 15(11). Available at: https://doi.org/10.3390/rs15112707.

Bouras, E.H. *et al.* (2021) “Cereal Yield Forecasting with Satellite Drought-Based Indices, Weather Data and Regional Climate Indices Using Machine Learning in Morocco,” *Remote Sensing*, 13(16), p. 3101. Available at: https://doi.org/10.3390/rs13163101.

Bourriz, M., Laamrani, A., *et al.* (2025) “Assessing hyperspectral sensor capabilities: PRISMA vs EnMAP for crop type mapping in a semi-arid region,” *Remote Sensing Applications: Society and Environment*, 40, p. 101815. Available at: https://doi.org/10.1016/j.rsase.2025.101815.

Bourriz, M., Hajji, H., *et al.* (2025) “Integration of Hyperspectral Imaging and AI Techniques for Crop Type Mapping: Present Status, Trends, and Challenges,” *Remote Sensing*, 17(9), p. 1574. Available at: https://doi.org/10.3390/rs17091574.

Bourriz, M. *et al.* (2026) “How Effective Are Foundation Models for Crop Type Mapping Using Hyperspectral Imaging? A Comparative Study of Machine Learning, Deep Learning, and Geospatial Foundation Models,” *The International Archives of the Photogrammetry, Remote Sensing and Spatial Information Sciences*, XLVIII-4/W17-2025, pp. 69–74. Available at: https://doi.org/10.5194/isprs-archives-XLVIII-4-W17-2025-69-2026.

El Hachimi, J. *et al.* (2022) “Assessment of the benefit of a single sentinel-2 satellite image to small crop parcels mapping,” *Geocarto International*, 37(25), pp. 7398–7414. Available at: https://doi.org/10.1080/10106049.2021.1974955.

Elbouanani, N. *et al.* (2025) “Enhancing Soil Fertility Mapping with Hyperspectral Remote Sensing and Advanced AI: A Comparative Study of Dimensionality Reduction Techniques in Morocco,” 15 March. Available at: https://doi.org/10.5194/egusphere-egu25-18418.

Hollmann, N. *et al.* (2025) “Accurate predictions on small data with a tabular foundation model,” *Nature*, 637(8045), pp. 319–326. Available at: https://doi.org/10.1038/s41586-024-08328-6.

Huang, X. *et al.* (2024) “A robust method for mapping soybean by phenological aligning of Sentinel-2 time series,” *ISPRS Journal of Photogrammetry and Remote Sensing*, 218, pp. 1–18. Available at: https://doi.org/10.1016/j.isprsjprs.2024.10.015.

Laamrani, A. *et al.* (2019) “Ensemble Identification of Spectral Bands Related to Soil Organic Carbon Levels over an Agricultural Field in Southern Ontario, Canada,” *Remote Sensing*, 11(11), p. 1298. Available at: https://doi.org/10.3390/rs11111298.

Meyer, H. *et al.* (2019) “Importance of spatial predictor variable selection in machine learning applications -- Moving from data reproduction to spatial prediction,” *Ecological Modelling*, 411, p. 108815. Available at: https://doi.org/10.1016/j.ecolmodel.2019.108815.

Misbah, K. *et al.* (2024) “Ensemble Band Selection for Quantification of Soil Total Nitrogen Levels from Hyperspectral Imagery,” *Remote Sensing*, 16(14), p. 2549. Available at: https://doi.org/10.3390/rs16142549.

Ouzemou, J.-E. *et al.* (2018) “Crop type mapping from pansharpened Landsat 8 NDVI data: A case of a highly fragmented and intensive agricultural system,” *Remote Sensing Applications: Society and Environment*, 11, pp. 94–103. Available at: https://doi.org/10.1016/j.rsase.2018.05.002.

Peña, M.A. and Brenning, A. (2015) “Assessing fruit-tree crop classification from Landsat-8 time series for the Maipo Valley, Chile,” *Remote Sensing of Environment*, 171, pp. 234–244. Available at: https://doi.org/10.1016/j.rse.2015.10.029.

Ruß, G. and Brenning, A. (2010) “Spatial Variable Importance Assessment for Yield Prediction in Precision Agriculture,” in P.R. Cohen, N.M. Adams, and M.R. Berthold (eds.) *Advances in Intelligent Data Analysis IX*. Berlin, Heidelberg: Springer Berlin Heidelberg (Lecture Notes in Computer Science), pp. 184–195. Available at: https://doi.org/10.1007/978-3-642-13062-5_18.

Schratz, P. *et al.* (2019) “Hyperparameter tuning and performance assessment of statistical and machine-learning algorithms using spatial data,” *Ecological Modelling*, 406, pp. 109–120. Available at: https://doi.org/10.1016/j.ecolmodel.2019.06.002.

Thenkabail, P.S., Lyon, J.G. and Huete, A. (eds.) (2018) *Hyperspectral Indices and Image Classifications for Agriculture and Vegetation: Hyperspectral Remote Sensing of Vegetation*. 2nd ed. CRC Press. Available at: https://doi.org/10.1201/9781315159331.